Rational Function Representation of Flap Noise Spectra including Correction for Reflection Effects

J. H. Miles*
NASA Lewis Research Center, Cleveland, Ohio

A rational function is presented for the acoustic spectra generated by deflection of engine exhaust jets for under-the-wing and over-the-wing versions of externally blown flaps. The functional representation is intended to provide a means for compact storage of data and for data analysis. The expressions are based on Fourier transform functions for the Strouhal normalized pressure spectral density, and on a correction for reflection effects based on the *N*-independent-source model of P. Thomas extended by use of a reflected ray transfer function. Curve fit comparisons are presented for blown flap data taken from turbofan engine tests and from large-scale cold-flow model tests. Application of the rational function to scrubbing noise theory is also indicated.

Nomenclature

$A_c(\Omega)$ = correlation area over which the normalized cross spectral density of the normal stress is unity
a_i = zero of $\phi(\Omega)$, $i=1, 2, \ldots, M_a$
a_0 = a complex number, normalization constant
b_k = pole of $\phi(\Omega)$, $k=1, \ldots, M_b$
C_e = cost function, sum of square of error between measured and calculated sound spectra
C_p = penalty function
C_T = total cost function
C_1, C_2, C_3 = cancellation frequencies
c = a complex number
c_0 = velocity of sound, m/sec
D_e = effective diameter, m
d_m = a complex constant, $m=1, 2, \ldots, K_d$
$F(c)$ = Strouhal response function
f = frequency, Hz
f_c = nominal mean frequency, Hz
$G(s)$ = reflected ray transfer function
$g(\tau)$ = reflecting surfaces' impulse reponse function
h_0 = microphone height, m
$h_s(n)$ = height of nth source, m
K_d = number of $\sigma(\Omega, d_m)$ terms in $A_c(\Omega)$ and $\psi(\Omega)$
ℓ = third-octave band number
M_a = number of numerator $\sigma(\Omega, a_i)$ terms of $\phi_{\text{real}}(\Omega)$
N = number of independent noise sources
N_b = number of denominator $\sigma(\Omega, b_k)$ terms of $\phi_{\text{real}}(\Omega)$
n = source index
OASPL = overall sound pressure level relative to p_r, db
OASPL_p^+ = lossless OASPL parametric value, db
PSD = Strouhal normalized mean-square pressure level, db
PSD^+ = *PSD without atmospheric absorption and ground reflection effects, db*
PSD^+ = PSD without atmospheric absorption and ground reflection effects, db
$\text{PSD}^+_{\text{cal}}$ = PSD^+ calculated from formula, db
PSD^+_{M} = PSD^+ calculated from measured data, db
$\text{PSD}^+_{\text{real}}(\Omega)$ = PSD^+ calculated from a real random process spectrum density, db
p = pressure, Pa
p' = reflected pressure signal, Pa
p_r = reference pressure 2×10^{-5} Pa (2×10^{-4} microbar)
$\lvert Q(s)\rvert$ = magnitude of reflected ray transfer function
R_2, R_3, R_4 = reinforcement frequency
r = distance from source to microphone, m
$S(x)$ = surface immersed in a flow
SPL = third-octave sound pressure level reference to p_r, db
SPL^+ = third-octave sound pressure level referenced to p_r that would be measured without atmospheric attenuation and in the absence of reflecting surface, db
SPL_{cal} = SPL calculated from an equation, db
SPL_m = SPL measured, db
St = Strouhal number, $f(D_e/V_e)$
St_0 = constant Strouhal number (0.3, Ref. 8)
s = $j2\pi f, j\omega$
s_1 = distance from source to microphone along direct ray path, m
s_2 = distance from source to microphone along reflected ray path, m
$\lvert T(f_c)\rvert^2$ = reflectance
t = time, sec
V_e = effective velocity, m/sec
x = surface position vector
z = mean ratio of path length reflected ray traveled to path length direct ray traveled for all n sources
α_0 = real constant, $-2\pi St_0$
Δf_c = bandwidth at center frequency f_c ($0.2316 f_c$), Hz
$\delta(s)$ = reflected ray transfer function phase factor, rad (deg)
θ = microphone angle relative to inlet
$\sigma(\Omega, c)$ = function of Strouhal number based on the reciprocal of the Fourier transform of a "damped oscillation" = $(\Omega-c)(\Omega-c^*)/(\Omega+(cc^*)^{1/2})$
τ = time delay, sec
τ_n = time delay between arrival of wave leaving source at time t and traveling direct path to receiver and one leaving at time t and traveling reflected ray path to receiver, sec
$\phi(\Omega)$ = Strouhal normalized mean-square pressure

Presented as Paper 74-193 at the AIAA 12th Aerospace Sciences Meeting, Washington, D.C., January 30-February 1, 1974; submitted February 25, 1974; revision received February 26, 1975.
Index category: Aircraft Noise, Aerodynamics (including Sonic Boom).
*Aerospace Engineer, Acoustics and Noise Division. Member AIAA.

$\phi_{real}(\Omega)$ = Strouhal normalized mean-square pressure for a real random process
$\psi(\Omega)$ = spectrum of the pseudosound or fluctuating surface pressure
Ω = relative angular velocity, $j2\pi f(D_e/V_e) = j2\pi St$
ω = angular velocity, $2\pi f$, rad/sec
j = $\sqrt{-1}$

Superscript

$(*)$ = *conjugate*

Introduction

FUTURE short takeoff and landing (STOL) aircraft will undoubtedly be required to meet stringent noise level regulations. Thus, noise is one of the primary factors in the selection of a STOL propulsion-lift system. One candidate source of propulsive-lift is the externally blown flap (EBF) system. Propulsive lift is generated by downward deflection of engine exhaust jets in either the under-the-wing or the over-the-wing version of EBF. Each EBF STOL concept introduces noise sources not present in conventional takeoff and landing (CTOL) airplanes which cause an increase in noise. These EBF STOL propulsive lift concepts are being investigated by scale-model tests,[1-4] and full scale engine tests.[5] Concurrently, theoretical and experimental studies are being conducted on various noise source mechanisms,[6-8] and empirical prediction methods are being devised.[9]

Many noise source mechanisms may contribute to the overall noise of an EBF system. These include 1) leading-edge noise caused by incident turbulence; 2) scrubbing noise generated in the turbulent boundary layer produced by the jet mixing region and convected along the wing or flap; 3) separated-flow noise; 4) trailing-edge noise caused by vortex shedding of eddies from the deflected flap; 5) jet mixing noise from the distorted deflected exhaust jet; and 6) engine internal and turbomachinery noise. Each of these sources may dominate at some angle depending on the specific jet exhaust velocity and EBF STOL configuration. The noise source mechanism receiving most emphasis is the one to which scrubbing noise is attributed.[10-12]

The objective of this paper is to determine a rational function representation of overall flap noise spectra that is useful 1) as an empirical equation to fit EBF STOL spectral data, and 2) as a function that can be related to certain noise-source mechanisms. The rational function representation is intended to serve as a link between experimental EBF spectral data and theoretical explanations, and to provide a mathematical expression for EBF noise spectra that can become part of an empirical prediction method.

This report describes an empirical rational function that can be used to represent the third-octave sound pressure level spectrum designated in this report by SPL. The function provides a representation for broadband SPL spectra. With the representation described, sound spectra can be stored in a computer in a compact form and comparison of large amounts of data from different experiments is facilitated. The representation can also be used to extrapolate data to untested conditions, which is useful in making estimates of the perceived noise level (PNL) and the effective perceived noise level (EPNL), and footprint calculations. In functional form, new relations or physical insights into source mechanisms may more easily become apparent. In fact, the empirical functional representation is related herein to a theoretical description of scrubbing noise, and thus provides a reason for the observed similarity of EBF data. In achieving this functional representation, corrections for acoustic reflections in ground test data are taken into account. Details of the development for the ground reflection correction have been published.[13]

The paper will present the development of equations representing the spectra. A basic equation is given in terms of the spectral density of a real random process. This equation will be related to scrubbing noise theory. Next, a simplified equation that represents the spectra will be given. Equations for corrections for reflection and atmospheric effects will also be included. The complete calculation method will then be discussed, and finally, results from EBF data taken from turbofan engine tests and cold-flow tests of under-the-wing test models will be given.

Analysis

Approach

The approach taken to represent flap noise spectra is based upon finding a function of Strouhal number $\phi(\Omega)$ such that the third-octave sound pressure level (SPL) can be fitted by Eq. (1)

$$\mathrm{SPL}^+(\ell) = 10\log_{10}\{[10^{\mathrm{OASPL}^+/10}] \times [\Delta f_c(\ell)\ (D_e/V_e)\ ]\ \phi(\Omega)\} \quad (1)$$

where

$$\mathrm{OASPL}^+ = 10\log_{10}[\Sigma_\ell\ 10^{\mathrm{SPL}^+(\ell)/10}] \quad (2)$$

The effective diameter D_e and the effective velocity V_e are as defined in Refs. 2, 3, and 9. The requirements on the function $\phi(\Omega)$ are: 1) It should be tailored for applicability to large Strouhal numbers. Curve fits that are accurate at large Strouhal numbers are necessary, since externally blown flap engines are likely to have large effective diameters and low exhaust velocities; 2) It should be consistent with theoretical considerations; 3) It should depend on as few mathematical coefficients and operations as possible, since this will reduce computer calculation time; and 4) It should be applicable to a wide range of system configurations (e.g., single or coannular nozzles, mixer nozzles, over-the-wing, and under-the-wing, etc.).

From Eq. (1)

$$10\log_{10}\{\phi(\Omega)\} = \mathrm{SPL}^+(\ell) - \mathrm{OASPL}^+ - 10\log_{10}[\Delta f_c(\ell)\ (D_e/V_e)\ ] = \mathrm{PSD}^+ \quad (3)$$

The quantity represented by Eq. (3) is the Strouhal normalized mean-square pressure spectral density level. In this paper, Eq. (3) will be referred to as the PSD^+ function. PSD^+, which is a function of Strouhal number, is calculated from SPL data free of atmospheric absorption and reflection effects (lossless data). It has been shown that spectral data taken over a range of exhaust velocities for numerous engine-over-the-wing and engine-under-the-wing externally blown flap configurations correlate when plotted in terms of the PSD^+ function (e.g., Refs. 1 and 2).

Spectral Density Function

Basic Function

The mathematical criteria that $\phi(\Omega)$ must satisfy to represent a power spectral density are that it must not be negative and must be integrable. However, to represent the power spectral density of a real random process, $\phi(\Omega)$ must also be an even function of Strouhal number. A basic function having these properties can be formulated from the reciprocal of the Fourier transform of a "damped cosine oscillation." Explicitly, the function is

$$\sigma(\Omega, c) = (\Omega - c)\ (\Omega - c^*)/[\Omega + (cc^*)^{1/2}] \quad (4)$$

The function $\sigma(\Omega,c)$ defines a curve of σ for a given value of c. Since the desired expression for $\phi(\Omega)$ involves the logarithmic addition of a number of individual $\sigma(\Omega,c)$ curves (to fit observed PSD^+ variation), the general expression for a

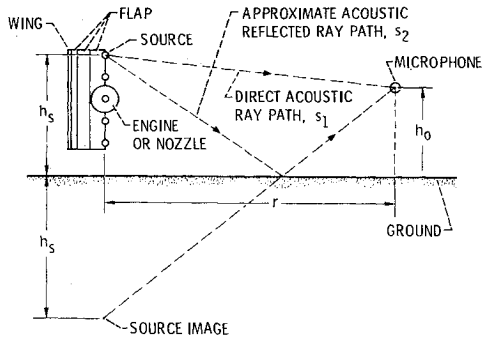

Fig. 1 Schematic of source and microphone geometry for test installation.

real random process, $\phi_{real}(\Omega)$, can be expressed as the ratio of the products of these terms

$$\phi_{Real}(\Omega) = \left| \left[a_0 \prod_{i=1}^{M_a} \sigma(\Omega, a_i) / \prod_{k=1}^{N_b} \sigma(\Omega, b_k) \right] \right|^2 \quad (5)$$

The complex numbers a_i and b_k have negative real values and positive or zero imaginary values, and M_a is less than N_b. The individual curves comprising the total function $\phi_{real}(\Omega)$ are referred to as Strouhal response functions.

Simplified Function

Equation (5) is the power spectral density of a real random process. A modification of Eq. (5) that yields a simpler expression, which is equally suitable for representing PSD$^+$ data, will be discussed next. However, while the new equation can be used to fit a spectral density satisfactorily, it does not represent a power spectral density of a real random process.

The modification consists of dropping the term $(\Omega - c^*)/[\Omega + (cc^*)^{1/2}]$ from Eq. (4). The equation for the calculated loss less PSD$^+$ then can be written as

$$\mathrm{PSD}^+_{cal} = 10 \log_{10} \left| \left[a_o \prod_{i=1}^{M_a} (\Omega - a_i) / \prod_{k=1}^{N_b} (\Omega - b_k) \right] \right|^2 \quad (6)$$

where all symbols are the same as in Eq. (5).

Application to Scrubbing Noise Theory

Equation (5) can also be used to yield inputs to a theoretical description of scrubbing noise. Starting from Curle's extension of Lighthill's theory to surfaces,[10] it is possible to show that dipole broadband noise is radiated from a rigid surface adjacent to a turbulent boundary layer. The noise produced is referred to as scrubbing noise. The Strouhal normalized mean-square pressure of this noise[11,12] would correspond to, in the notation of this paper

$$\phi(\Omega) = \frac{|\Omega|^2 \int_S \psi(\Omega) A_c(\Omega) \mathrm{d}S(x)}{(2\pi)^2 \int_0^\infty St^2 \int_S \psi(\Omega) A_c(\Omega) \mathrm{d}S(x) \mathrm{d}St} \quad (7)$$

Some attempts have been made to define equations for $\psi(\Omega)$ and for $A_c(\Omega)$ based on experimental data for surfaces other than flaps.[11,12] The necessary measurements do not exist specifically for flap noise sources. However, empirical representations of the $\psi(\Omega)$ and $A_c(\Omega)$ functions for flap noise have been made based on experimental data of similar phenomena. In Ref. 8, Fink approximated the correlation area (in the notation of this paper) by

$$A_c(\Omega) = |2\pi / (\Omega - \alpha_0)|^2 \quad (8a)$$

and the static pressure fluctuation spectrum was approximated by

$$\psi(\Omega) = |2\pi(\Omega - \alpha_0) / [(\Omega - b_1)(\Omega - b_2)]|^2 \quad (8b)$$

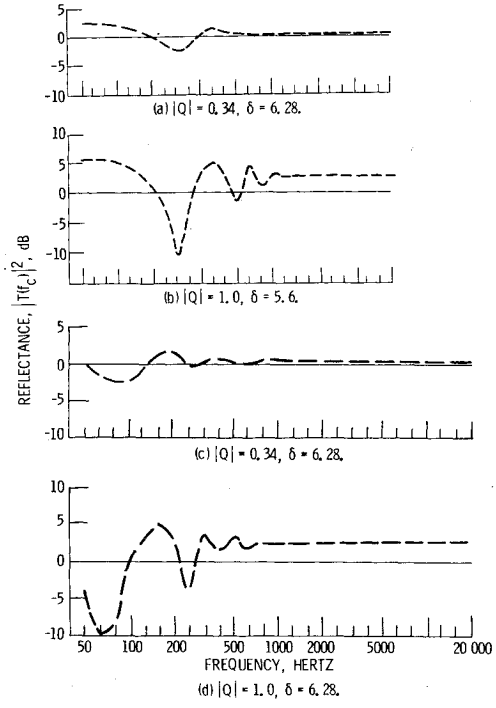

Fig. 2 Calculated reflectance [Eq. (12)]: 1) for cold-flow-blown flap data site (Ref. 2): a) $|Q| = 0.34$, $\delta = 6.28$; b) $|Q| = 1.0$, $\delta = 5.6$; 2) for turbofan engine externally blown-flap data site (Ref. 5): c) $|Q| = 0.34$, $\delta = 6.28$; d) $|Q| = 1.0$, $\delta = 6.28$.

where

$$b_1 = \pi St_0 \sqrt{2}\,(-1-j)$$

$$b_2 = \pi St_0 \sqrt{2}\,(-1+j)$$

More general and flexible expressions for these two functions can also be postulated from Eq. (5) as follows

$$A_c(\Omega) = \left| \left[\prod_{i=1}^{M_a} \sigma(\Omega, a_i) / \prod_{m=1}^{K_d} \sigma(\Omega, d_m) \right] \right|^2 \quad (9a)$$

$$\psi(\Omega) = \left| \left[\prod_{m=1}^{K_d} \sigma(\Omega, d_m) / \prod_{k=1}^{N_b} \sigma(\Omega, b_k) \right] \right|^2 \quad (9b)$$

where $M_a < K_d < N_b$, and d_m has a negative real part and a zero or positive imaginary part.

Reflection Correction

Acoustic reflections cause problems with experimental SPL data. In some experiments, reflections distort the true sound spectrum, which leads to incorrect spectral shapes and a frequent overestimation of the overall sound pressure level (OASPL). A typical acoustic test geometry having ground reflections is the test geometry used for evaluating the noise from the engine under-the-wing EBF configuration shown in Fig. 1.

The measured sound pressure level is given by

$$\mathrm{SPL}(f_c) + \mathrm{SPL}^+(f_c) + 10 \log |T(f_c)|^2 \quad (10)$$

where $|T(f_c)|$ is the reflectance and $\mathrm{SPL}^+(f_c)$ is the sound pressure level without atmospheric attenuation and ground reflection. Equation (10) is arrived at by assuming the noise source is distributed over a region and is represented by signals from N independent equal strength sources. This assumption was used by Thomas[14] to study acoustic interference of the noise produced by a single jet due to reflections from a plane surface. The ground reflection effect on a single-point noise source has already been treated.[15,16]

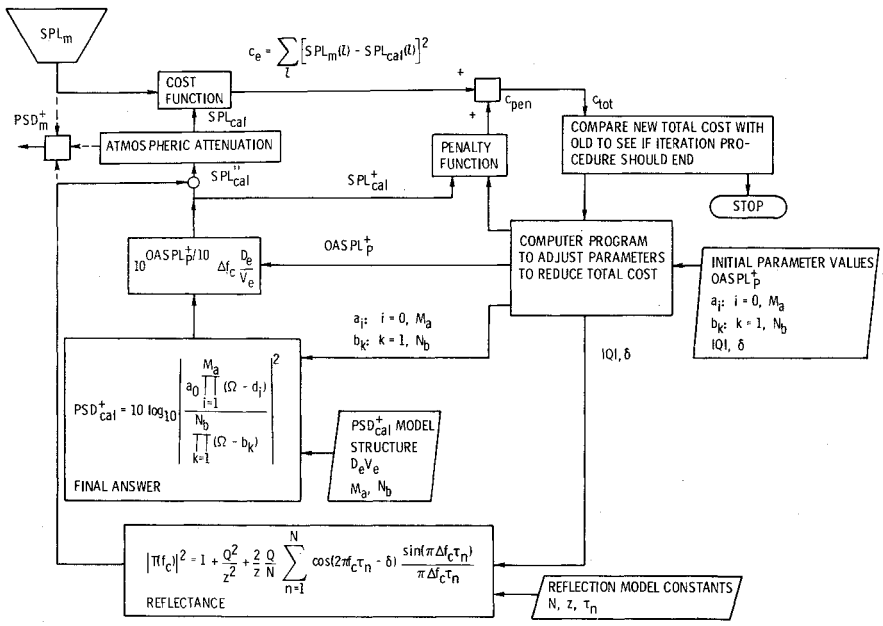

Fig. 3 Diagram of computer method.

Table 1 Constants used in reflectance calculations

a) Constants used for reflectance shown in Figs. 2a and 2b. $N=5$; $r=15.24$ m (50 ft); $h_m=3.88$ m (12.75 ft)

n		1	2	3	4	5
$h_s(n)$	m	4.130	4.0081	3.886	3.764	3.642
	ft	13.55	13.15	12.75	12.35	11.95
τ_n	sec	0.0058	0.00567	0.0055	0.0053	0.0052

b) Constants used for reflectance shown in Figs. 2c and 2d. $N=5$; r = 30.48 m (100 ft); $h_m=2.74$ m (9 ft)

n		1	2	3	4	5
$h_s(n)$	m	3.475	3.736	2.743	2.377	2.012
	ft	11.4	10.2	9.0	7.8	6.6
τ_n	sec	0.00182	0.00164	0.00145	0.00125	0.00106

In calculating the reflectance, the reflected pressure signal is assumed to be related to the direct pressure signal by a convolution of the reflecting surfaces' impulse response $g(\tau)$ with the direct pressure signal. The Laplace transform of the reflecting surfaces' impulse response is the reflected signal transfer function $G(s)$. This complex reflected ray transfer function can be written in terms of its phase $\delta(s)$ and amplitude $|Q(s)|$. The approximation found most useful in specifying $G(s)$ was to assume that $|Q(s)|$ and $\delta(s)$ are constant over the frequency range of interest. Thus

$$G(s) = |Q|e^{j} \tag{11}$$

The reflectance calculated from these assumptions is

$$|T(f_c)|^2 = 1 + [|Q|^2/z^2] + (2/N)(|Q|/z)\sum_{n=1}^{N} \cos(2\pi f_c \tau_n - \delta)\,\frac{\sin(\pi \Delta f \tau_n)}{\pi \Delta f \tau_n} \tag{12}$$

Typical reflectances for a low and high level of $|Q|$ are shown in Fig. 2. Figures 2a and 2b apply to the test configuration at the cold-flow model test site,[2] and Figs. 2c and 2d apply to the test configuration at the EBF test site.[5] Table 1 contains the values of the constants used in the reflectance calculations. The effect of low $|Q|$ values is to minimize the magnitude of the cancellations and reinforcements.

Calculation Method

The complete equation used to represent the SPL at a microphone for a given source/microphone geometry is based on Eqs. (1, 3, 6, 10, and 12) and an atmospheric attenuation computed by the method of Ref. 17. Components of the resulting equation are shown in Fig. 3 as part of a computer method used to adjust simultaneously the reflection model parameters Q and δ and the functional representation parameters [Eq. (6)] to fit measured data. Since the calculated SPL depends on both sets of parameters, in situations where the acoustic reflection model parameters are unknown, the functional representation plays a vital part in correcting reflection effects.

A computer program is used to adjust the parameters OASPL^{+}_{p}, a_0, a_i; $i=1, \ldots, M_a$, b_k; $k=1, \ldots, N_b$, $|Q|$ and δ. A diagram of the method is shown in Fig. 3. The parameters are adjusted to minimize the total "cost" C_T, consisting of the sum of the squares of the differences between the measured and calculated SPL values C_e and a penalty cost[18] C_p, due to selection of parameters that violate the parameter constraints previously mentioned. [See Eq. (2) for OASPL^{+}_{p} constraint and Eq. (5) for a_i and b_k constraint.] The total cost function is nonlinear. The problem of minimizing the nonlinear cost function was solved by search techniques. These techniques consist of systematic procedures for varying the cost function parameters until a minimum value of the cost function is found. The basic methods available are discussed in Ref. 18. To provide flexibility, a search technique which does not require evaluation of derivatives was chosen. The search technique was that of Powell.[19] The computer program used was adapted from Ref. 20.

The input information for the method consists, first, of the constants required for the reflection model. These consist of the following: the number of sources N, which was selected to be 5; the mean value of the ratio of the distance the reflected ray travels to the distance the direct ray travels z; and the time delay τ_n associated with each of the five sources. Second, the constants M_a and N_b for the $\text{PSD}^{+}_{\text{cal}}$ model are needed. For the data considered N_b was selected to be 3 and M_a was selected to be 1. Last, initial values of the parameters to be varied (OASPL^{+}_{p}, a_0, $|Q|$, δ, a_1, b_1, b_2, b_3) are necessary.

Results

Basic PSD^{+} Function

Several sets of lossless blown flap data are available for determining fits by the PSD^{+} function based on the formulation for a real random process given by Eq. (5). Data correlations over a range of exhaust velocities in terms of lossless spectral density vs Strouhal number are available[1] for

Table 2 Parameters to calculate selected PSD^{+}_{real} curves using Eqs. (4) and (5)

Dimensionless parameter	Complex number C (real value, imaginary value), $C=a_0, a_1, b_1, b_2$, or b_3 Data of Fig. 4a	Data of Fig. 4b
a_0	(151.610, 151.610)	(133.3510, 133.3510
a_1	(−0.1965826, 0.1824718)	(−0.1304851, 0.1214311)
b_1	(76.22998, 26.7030)	(−0.1540204, 0.4026451)
b_2	(−0.9577132, 0.7647091)	(−1.564607, 1.282075)
b_3	(−1.546595, 2.192013)	(−76.433486, 35.98859)

Table 3 Parameters to calculate selected PSD^{+}_{cal} curves using Eq. (6)

Dimensionless parameter	Complex number C (real value, imaginary value), $C=a_0, a_1, b_1, b_2$, or b_3 Data of Fig. 4a	Data of Fig. 4b
a_0	(192.6902, 192.6902)	(105.7856, 105.7856)
a_1	(−0.2528992, 0.1505393)	(−0.1947860, 0.06866252)
b_1	(−1.194895, 0.5249010)	(−0.1479430, 0.4224659)
b_2	(−1.745644, 1.715307)	(−1.963396, 1.474141)
b_3	(−115.7714, 14.24272)	(−73.48344, 45.69005)

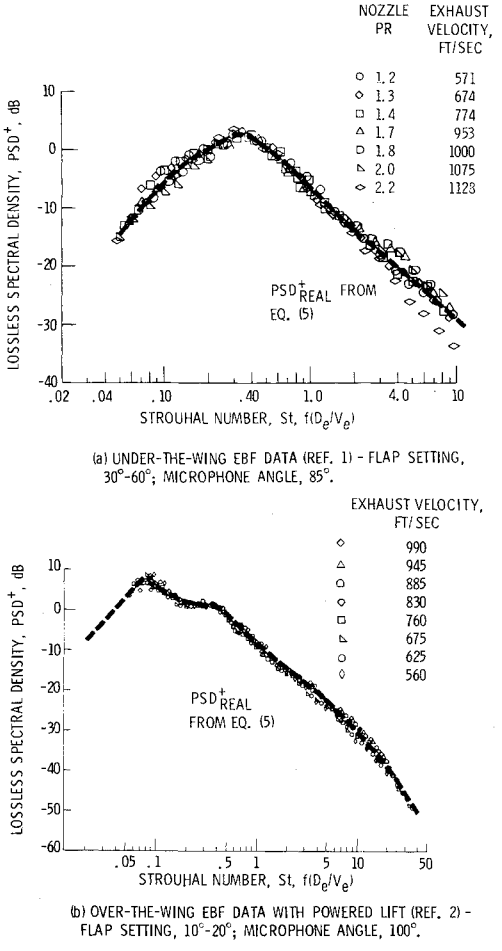

Fig. 4 Comparison of curve fit using Eq. (5) with Strouhal correlation of lossless data.

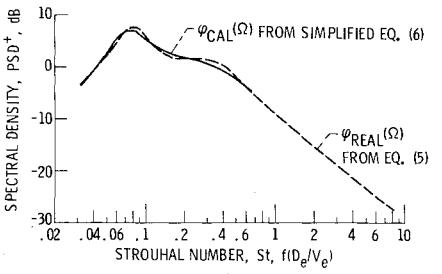

Fig. 5 Basic and simplified spectral density functions used to fit lossless data of Fig. 4b.

a cold-flow test of an under-the-wing externally blown flap configuration. Comparable Strouhal correlations for a cold-flow over-the-wing configuration with attached flap flow (powered lift) and with unattached flow (conventional lift) are presented in Ref. 2. Calculated values of PSD^{+} for these data were obtained from iterative calculations of Eqs. (5) and (3) in conjunction with the measured values of PSD^{+}. A total of nine parameters was used in the calculation. The parameter values corresponding to the best fit of the data are given in Table 2.

Figure 4a shows a comparison of the data and the curve fit for PSD^{+} for the under-the-wing model of a flap setting of 30°-60° for the 85° microphone angle position. Figure 4b shows a comparable comparison at a microphone angle of 100° above an over-the-wing model with attached flow at a flap setting of 10°-20°. In both cases, the calculated curve fits are in very good agreement with the data over the entire Strouhal number range. Thus, Eq. (5) should be applicable to data from many different types of blown flap configurations. Equation (5) was successfully applied to data from an over-the-wing model with unattached flow at flap settings[21] of 10°-20° and 30°-60°.

Simplified PSD Function

The simplified PSD^{+} function of Eq. (6) was also used to fit the data shown in Fig. 4. The nine parameters obtained are shown in Table 3 in terms of the complex constants needed for the fit. In all cases, the curve fit to the data was very nearly as good as for the basic function of Eq. (5). An example of the comparison is given in Fig. 5, which shows the calculated PSD^{+} values for the basic [Eq. (5)] and simplified [Eq. (6)] functions are obtained for the fit of the data of Fig. 4b. On the basis of the close correspondence of the two results, it was concluded that the simplified version of the PSD^{+} function given by Eq. (6) is completely adequate for routine calculation purposes.

Number of Parameters

The curve fits used in fitting the data shown in Fig. 4 were based on using $M_a=1$ and $N_b=3$, which results in nine parameters in Eqs. (5) and (6). Calculation of the individual

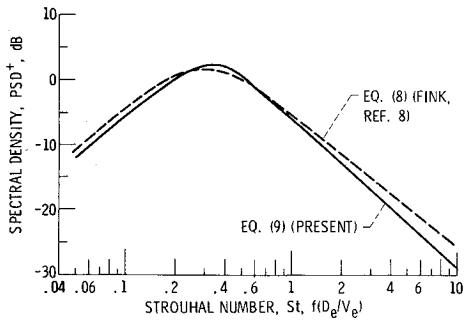

Fig. 6 Plot of PSD$^+$ functions based on data shown in Fig. 4a.

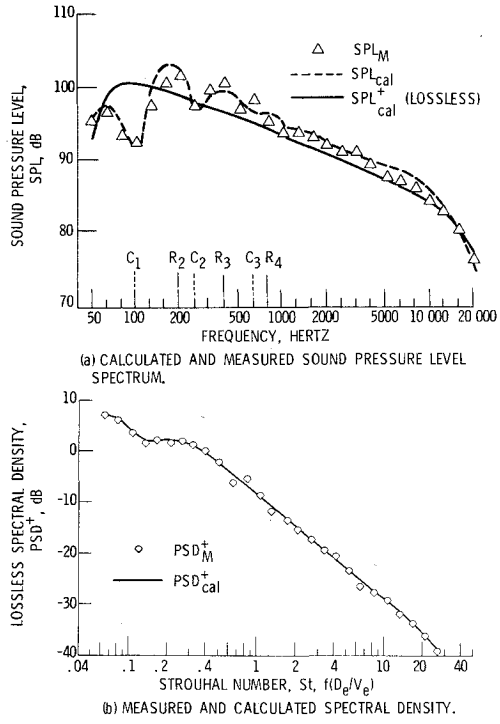

Fig. 7 Spectral characteristics of over-the-wing cold-flow powered lift model with flap position 10°-20° (Ref. 2). Exhaust velocity, 253 m/sec; distance 15.2 m; microphone height, 3.9 m; source height, 3.9 m; microphone angle, 100°.

Strouhal response functions $F(a_1)$, $F(b_1)$, $F(b_2)$, $F(b_3)$ corresponding to a_1, b_1, b_2, and b_3 that make up the simplified PSD$^+$ functions of Fig. 5 indicate the $F(b_3)$ curve does not contribute to the final curve form. Consequently, a seven-parameter formulation of Eqs. (5) or (6) should be adequate for many calculations.[21]

Application to Scrubbing Noise Theory

The functional form of $\phi(\Omega)$ based on Eqs. (7, 8a, and 8b) as developed by Fink[8] for scrubbing noise is a three-parameter function. A second functional form developed herein, represented by Eq. (5), can be related to scrubbing noise, using Eqs. (7, 9a, and 9b), which involve seven parameters. Assuming scrubbing noise is the major contributor to overall noise, the ability of the two different functional forms of $\phi(\Omega)$ to fit the data shown in Fig. 4a can be compared.

Figure 6 shows the comparison between the curves derived From Eq. (7) and (9) [identical to the use of Eq. (5)] and from Eqs. (7) and (8) with $St_0 = 0.3$ for the data of Fig. 4a. As previously discussed, the curve based on Eq. (5) using seven parameters provides a very good fit to the data, as shown in Fig. 4a. The three-parameter functional form of $\phi(\Omega)$ derived by Fink is seen in Fig. 6 to be in general agreement with the form derived herein (and thus with the data of Fig. 4a), but it

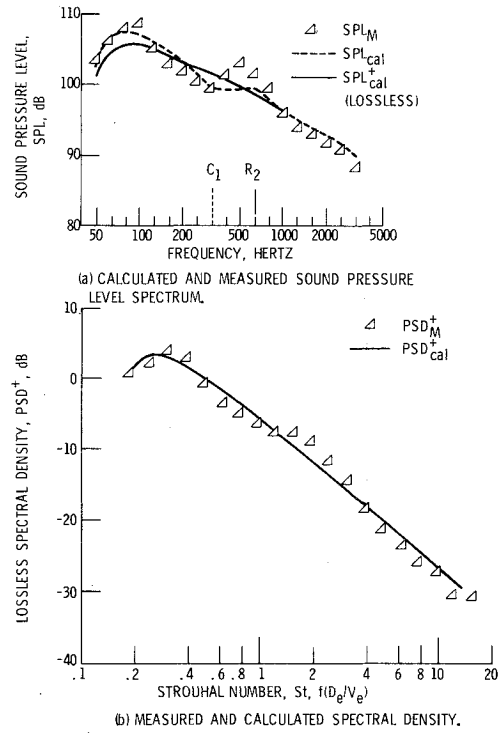

Fig. 8 Spectral characteristics of turbofan engine externally blown-flap configuration with effective exhaust velocity, 242 m/sec; distance 30.43 m; microphone and source height, 2.74 m; microphone angle, 80°.

overestimates the PSD$^+$ at large Strouhal numbers. This overestimation was recognized by Fink[8]

Thus, the assumption that scrubbing noise is a major contributor to overall noise can be supported by the functional form developed herein. However, since the same functional form as Eq. (5) for the PSD$^+$ function from the other source mechanisms may produce a curve that can be fitted by Eq. (5), the excellence of the curve fit by itself does not necessarily prove that scrubbing noise is the major contributor to the overall noise.

Application to Measured Data

Cold-Flow Model

Original measured and calculated values are compared in Fig. 7 for a number of calculated quantities for the case of data from an over-the-wing model (Ref. 2) with two wing flaps and attached flap flow (powered lift configuration). The test configuration is for cold flow with a circular nozzle and a flap settting of 10°-20°.

Figure 7a shows the measured third-octave sound pressure level spectrum. The data were taken at an exhaust velocity of 253 m/sec (830 fps) and a microphone angle of 100° from the inlet. The cancellations denoted by C_1, C_2, C_3 and the reinforcements denoted by R_2, R_3, R_4 are due to reflection effects. Figure 7a also shows the measured sound pressure level, SPL_M, the calculated SPL, including effects of atmospheric absorption and reflections, SPL_{cal}, and the calculated lossless sound pressure level, SPL^+_{cal}. The reflectance used to account for the reflection effect is that shown in Fig. 2b. Comparison between measured (SPL_M) and calculated (SPL_{cal}) spectra indicates that SPL_{cal} gives a good fit to the data.

Figure 7b illustrates the fit between calculated values of lossless spectral density PSD^+_{cal} and the PSD$^+$ spectrum obtained from the measured SPL by using the calculated reflectance shown in Fig. 2b and a calculated atmospheric attenuation. This calculated PSD based on the measured SPL data is denoted as PSD^+_M. The close proximity of the least-square curve fit, PSD^+_{cal}, to the PSD^+_M calculated points is apparent.

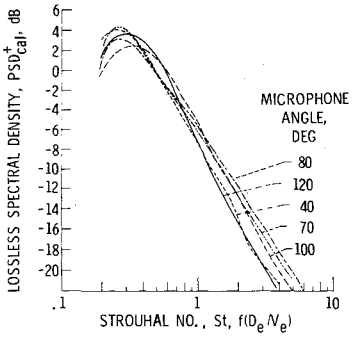

Fig. 9 Variation of lossless overall sound pressure level at effective velocity of 242.3 m/sec with microphone angles of 20°-140° for turbofan engine EBF configuration. Flap setting 0°-20°-40°; microphone radius, 30.48 m.

Full-Scale Engine Configuration

Another example of the application of the method is given for a set of data from the tests of Ref. 5 for a full-scale EBF system with a three-flap wing and a turbofan engine with a coannular nozzle. The test condition is for a takeoff flap setting of 0°-20°-40°, an effective exhaust velocity of 242.3 m/sec (795 fps) (maximum power), and a microphone angle of 80° from the inlet. Fig. 8a shows the measured third-octave SPL spectrum for the test condition. Reflection effects are indicated by the first cancellation denoted by C_1 and by the second reinforcement denoted by R_2. The turbofan engine in this program was highly noise suppressed with much of the fan discrete tone noise removed. However, because some residual fan tone noise may be present at frequencies above 4000 Hz for the maximum-power operating test condition only data from 50 to 3150 Hz were analyzed herein.

The calculated spectrum for lossless sound pressure level SPL^+ is shown in Fig. 8a. Also shown are calculated values of SPL, including reflection and atmospheric attenuation effects SPL_{cal}, and values of the measured sound pressure spectrum, SPL_M. The reflectance used to account for the reflection effects is similar to that shown in Fig. 2c. Comparison of SPL_{cal} with the measured SPL data SPL_M, indicates a good representation of the data was achieved. Figure 8b illustrates the fit between PSD^+_M and PSD^+_{cal}. A good least-squares curve fit was again achieved.

Variations with Angle and Velocity

Calculations were also made with the iteration method developed using data from the full-scale engine EBF configuration previously discussed, taken at microphone angles of 20°-140° over a range of exhaust velocities. For microphone angles between 20° and 90° the $OASPL^+_p$ varies with the sixth power of the effective exhaust velocity, reflecting the dominance of surface scrubbing (or dipole) noise. For angles between 100° and 140°, the data indicated a trend toward an eighth-power dependence on effective velocity. At 120° the eighth-power relation fits the data quite well. This is interpreted to be an indication that the jet (or quadruple mixing) noise source is more important at these greater angles.[13,21] Figure 9 shows PSD^+_{cal} for angles of 40°-120° at the maximum-power setting with $V_e = 242$ m/sec (795 fps). The curves for microphone angles of 40°-80° (sixth power of velocity region) are similar in appearance and peak at a Strouhal number between 0.25 and 0.27. The PSD^+_{cal} curves for microphone angles of 100° and 120° (eighth power of velocity region) have their peak values at a Strouhal number between 0.30 and 0.35. All the PSD^+ curves fall within a band of less than 4-db width.

Conclusions

A calculation procedure based on a simple rational function for spectral density has been shown to provide a representation for the acoustic spectra generated by deflection of engine exhaust jets for under-the-wing and over-the-wing versions of externally blown flap configurations. The representation is useful in correcting reflection effects, and provides a compact method of storing sound spectral data. In addition, the simple function is related to a more basic pressure spectral density function that can also be used to fit PSD data and can be related to scrubbing noise theory. The simple rational function combined with the procedure for correcting reflection effects yields mean-square pressure level per unit Shrouhal member curves that are devoid of interference effects and can be easily compared with one another.

References

[1] Dorsch, R. G., Kreim, W. J., and Olsen, W. A. "Externally Blown Flap Noise," AIAA Paper 72-129, San Diego, Calif., 1972

[2] Reshotko, M., Goodykoontz, J. H., and Dorsch, R. G., "Engine over-the-Wing Noise Research," *Journal of Aircraft*, Vol. 11, April 1974, pp. 195-196.

[3] Dorsch, R. G., Goodykoontz, J. H., and Sargent, N. B., "Effect of Configuration Variation on Externally Blown Flap Noise," AIAA Paper 74-190, Washington, D. C., 1974.

[4] Goodykoontz, J. H., Dorsch, R. G., and Wagner, J. M., "Acoustic Characteristics of Externally Blown Flap Systems with Mixer Nozzles," AIAA Paper, 74-192, Washington, D. C., 1974.

[5] Samanich, N. E., Heidelberg, L. J., and Jones, W. L., "Effect of Exhaust Nozzle Configuration on Aerodynamic and Acoustic Performance of an Externally Blown Flap System with a Quiet 6:1 Bypass Ratio Engine," AIAA Paper 73-1217, Las Vegas, Nev., 1973.

[6] Olsen, W. A., Dorsch, R. G., and Miles, J. H., "Noise Produced by a Small-Scale, Externally Blown Fap," NASA TN D-6636, 1972.

[7] Hayden, R. E., "Noise from Interaction of Flow with Rigid Surfaces: A Review of Current Status of Prediction Techniques," NASA CR-2126, 1972.

[8] Fink, M. R., "Mechanisms of Externally Blown Flap Noise," *AIAA Progress in Astronautics and Aeronautics: Aeroacoustics: Fan, STOL, and Boundary-Layer Noise; Sonic Boom; Aeroacoustics Instrumentation*, Vol. 38, edited by H. T. Nagamatsu, associate editors: J. V. O'Keefe, I. R. Schwartz, MIT Press, Cambridge, Mass., 1975, pp. 113-128.

[9] Clark, B. J., Dorsch, R. G., and Reshotko, M., "Flap Noise Prediction Method for a Powered Lift System," *AIAA Progress in Astronautics and Aeronautics: Aeroacoustics: Fan, STOL, and Boundary-Layer Noise; Sonic Boom; Aeroacoustics Instrumentation*, Vol. 38, edited by H. T. Nagamatsu, associate editors: J. V. O'Keefe, I. R. Schwartz, MIT Press, Cambridge, Mass., 1975, pp. 99-112.

[10] Curle, N., "The Influence of Solid Boundaries upon Aerodynamic Sound," *Royal Society (London), Proceedings, Series A*, Vol. 231, No. 1187, Sept. 1955, pp. 505-513.

[11] Sharland, I. J., "Sources of Noise in Axial Flow Fans," *Journal of Sound and Vibration*, Vol. 1, No. 3, 1964, pp. 302-322.

[12] Vecchio, E. A. and Wiley, C. A., "Noise Radiated from a Turbulent Boundary Layer," *Journal of the Acoustical Society of America*, Vol. 53, Feb. 1973, pp. 569-601.

[13] Miles, J. H., "Method for Representation of Acoustic Spectra and Reflection Corrections Applied to Externally Blown Flap Noise," NASA TM X-3179, 1975.

[14] Thomas, P., "Etude des Interferences Acoustiques Par Reflexion Applecation Aux Spectres de Pression Acoustique des Jets," *Aircraft Engine Noise and Sonic Boom*, AGARD-CP-42, St. Louis, France, May 27-30, 1969, pp. 10-17.

[15] Howes, W. L., "Gound Reflection of Jet Noise," NASA TR-35, 1959.

[16] Hoch, R. and Thomas, P., "Influence of Reflections on the Spectra of Acoustic Pressure of Jets," *Aeronautical Acoustical Symposium*, Toulouse, March, 1968.

[17] Evans, L. B. and Sutherland, L. C., "Absorption of Sound in Air," WR-70-14, July 1970, Wyle Labs., Huntsville, Ala.

[18] Pierre, D. A., *Optimization Theory with Applications*, Wiley, New York, 1969.

[19] Powell, M. J. D., "An Efficient Method for Finding the Minimum of a Function of Several Variables without Calculating Derivatives," *Computer Journal*, Vol. 7, July 1964, pp. 155-162.

[20] Shapero, M. S. and Goldstein, M., "A Collection of Mathematical Computer Routines," NYO-1480, Feb. 1965, New York University, New York.

[21] Miles, J. H., "Rational Function Representation of Flap Noise Spectra Including Correction for Reflection Effects," NASA TM X-710502, 1975.